



**Published:** February 29, 2024

**Citation:** Frayne EG, 2024. The Early Consequences of Thiophosphate Substitution in Escherichia coli: Possible Epigenetic and Energetic Factors, Medical Research Archives, [online] 12(2). <https://doi.org/10.18103/mra.v12i2.5089>

**Copyright:** © 2024 European Society of Medicine. This is an open-access article distributed under the terms of the Creative Commons Attribution License, which permits unrestricted use, distribution, and reproduction in any medium, provided the original author and source are credited.

**DOI**

<https://doi.org/10.18103/mra.v12i2.5089>

**ISSN:** 2375-1924

RESEARCH ARTICLE

## Early Consequences of Thiophosphate Substitution in Escherichia coli: Possible Epigenetic and Energetic Factors

**Elizabeth G. Frayne, PhD**

College of General Studies, University of Phoenix, Phoenix, AZ

Email: [efrayne@email.phoenix.edu](mailto:efrayne@email.phoenix.edu)

### ABSTRACT

Substitution of thiophosphate for phosphate during the culture of Escherichia coli leads to an increase in biosynthetic activity across a broad spectrum of pathways. To investigate the basis for this enhanced profile, early analysis of RNA transcripts was performed using RNA seq methods. The results identified a possible mediator of activation, namely the ser/thr kinase, yegl, which was increased ~190X fold during the first 1 hr. of induction. There is also a massive shift in the amount of non-ribosomal RNA relative to rRNA of 8-10X fold. RNA seq analysis further supports the idea that energy savings from reduced RNA turnover in thiophosphate treated cells, is the driving force for triggering the enhanced transcriptional profile in Escherichia coli. Thus, in response to an increased energy state, the cells appear to activate a new transcriptional program via a protein kinase cascade.

## Introduction

Thiophosphate, a phosphate analogue, can be used to enhance cellular biosynthesis and thereby serve as a potential archetype for cell differentiation<sup>1,2</sup>. The analogue likely induces these changes by increasing the cellular energy charge or state in simple cells like bacteria. A role for cellular energy in regulating differentiation is suggested by studies employing hypoxia or energy rich metabolites in mammalian cells<sup>3,4,5</sup>. Thus, metabolism itself has the potential to initiate or promote differentiation rather than simply respond to increased cellular demands.

Thiophosphate reduces RNA turnover by creating phosphorothioate linkages in RNA that inhibit cellular nucleases. The energy savings from reduced RNA turnover in Escherichia coli (E. coli) appears to enable an enhanced biosynthetic profile the result of transcriptional changes rather than differential mRNA stabilization<sup>1,2</sup>. Previous studies demonstrate that biosynthetic activity at later stages of growth show enhancements in the transcription of genes for RNA processing enzymes, ribosomal proteins, tRNA charging enzymes, translational proteins, as well as outer membrane, plasma membrane, and periplasmic proteins<sup>1</sup>. Furthermore, there are also increases in transcripts for genes involved in the synthesis of amino acids, fatty acids, carbohydrates, cell structures, cofactors, vitamins, and secondary metabolites, etc. However, it is unclear how these changes in gene activity are linked to the presumed changes in cellular energy.

The present study exams early time points during the culture of E. coli with thiophosphate as a phosphate analogue. The results revealed insight into possible epigenetic and energetic mechanisms responsible for the enhanced biosynthetic activity observed by late log. Interestingly, after only 1 hr. of incubation transcripts for a ser/thr kinase were increased 190X fold in thiophosphate treated cells. This enzyme could serve as a link between the cellular energy charge and the increased biosynthetic activity via a kinase cascade.

## Methods

E. coli cells were cultured in M9 minimal media or semisynthetic media. M9 was made with 1.5 g/L KCL for a potassium source along with 5 g/L of

sodium thiophosphate freshly dissolved and sterile filtered. The semisynthetic media used contained glucose, 60 g/L; KCL 0.8 g/L; MgSO<sub>4</sub> 0.4 g/L; peptone, 2 g/L; NH<sub>4</sub>Cl 8 g/L, urea, 3 g/L, calcium chloride, 0.2 g/L. Thiophosphate was then added at 2.7 g/L, while controls had 1 g/L NaH<sub>2</sub>P<sub>0</sub>4. Cells were suspended in RNA Shield™ and immediately placed on dry ice for RNA isolation using Omega Biotek's E.S.N.A. RNA isolation kit. RNA was quantified using nanodrop analysis and the integrity assessed using RNA Screentape<sup>6</sup>.

RNA seq analysis was performed as described previously<sup>1</sup>, except that rRNA was removed from samples using RiboZero Plus™ prior to stranded mRNA library preparation. Illumina sequence was performed at 20 million PE Reads (10M in each direction). The read format was PE 2 X 150 bp. Differential expression analysis was performed using E. coli K12 substr. MG1655 as the reference genome. The EcoCyc database along with the Omics data analysis software was used to further analyze the RNA seq data in terms of biochemical pathways<sup>7</sup>. GC content analysis of the E. coli genome was performed using NCBI genome work bench version 3.5.0<sup>8</sup> and screening for GC islands of at least 130 bp.

## Results

### TIME COURSE TO STEADY STATE

Changes in the pattern of mRNA synthesis could be observed directly in Agilent gels of total RNA from E. coli treated with or without thiophosphate (Fig. 1). By quantifying scans of the gels, a 25-30% increase in non-ribosomal RNA was seen at 1 hr. suggesting an 8-10X fold increase in E. coli mRNA. By 5 hrs. this increase is reduced ~50% and stayed that way reaching a new steady state relative to controls. Note in late log cells, a 4-6X fold increase is also seen in RNA seq data<sup>1</sup>. Cells from late log were also simply resuspended for the time periods indicated. The results (Fig. 1) suggested that cells do not need to be growing to have the effect. Analysis of cell growth indicates that cells do not grow during the initial 1 hr. incubation period as they adjust to the analogue. However, after that they resume cell growth (unpublished observations). Similar results are seen with tryptic soy broth and Luria broth media.

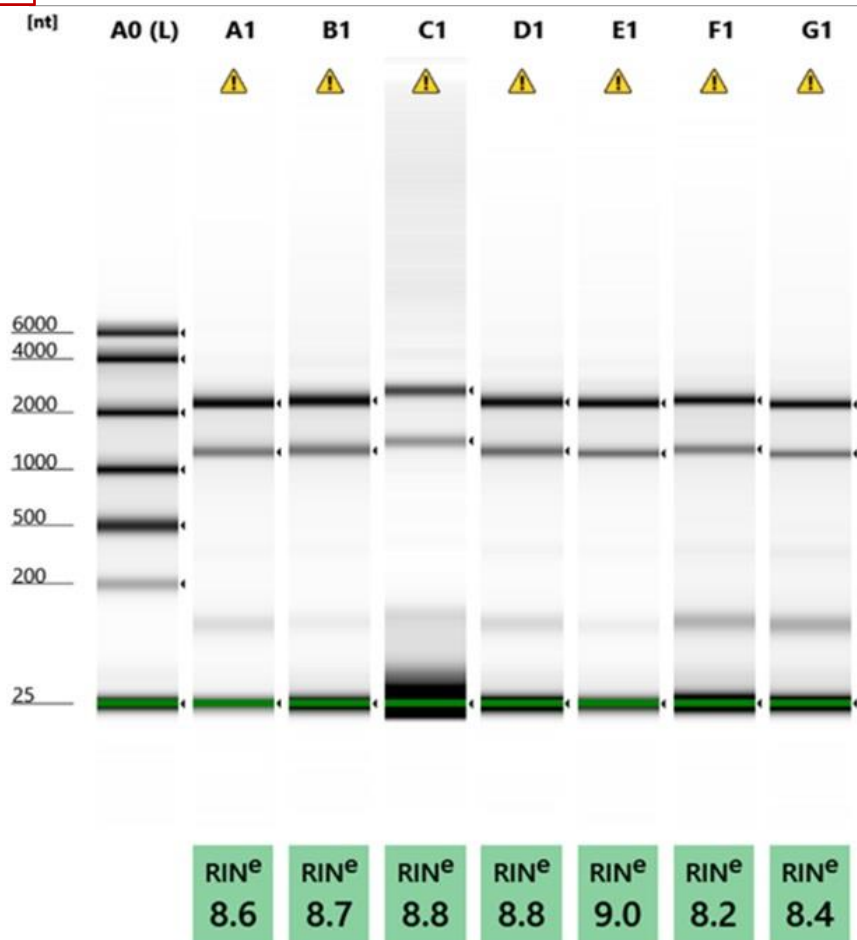


**Figure 1.** Agilent gel analysis of total RNA isolated from cells treated with thiophosphate using synthetic and semisynthetic media. A1 shows control cells in semisynthetic media, B1 & C1 show cells grown for 1 hr. with thiophosphate using respectively M9 or semisynthetic media. D1 shows cells resuspended in semisynthetic thiophosphate media for 1 hr. E1 & F1 show cells grown for 5 hrs. with thiophosphate using respectively M9 or semisynthetic media. G1 shows cells resuspended in semisynthetic media with thiophosphate for 5 hrs. Note B1 and E1 are results using M9 media and the rest using semisynthetic media.

#### EARLY IMPACTS ON GENE EXPRESSION

RNA seq analysis revealed that 3,200 *E. coli* genes could be detected after depleting rRNA in samples prior to analysis. In thiophosphate treated cells 735 genes were enhanced an average of 8.4X fold (SD 13.4) with a median of 4. Also 157 gene transcripts showed a mean and median decrease of 2X fold (SD 3.7). Notably 2,309 were not detected in

thiophosphate treated samples. The massive increase in non-ribosomal RNA made it difficult to detect many gene transcripts in treated samples via RNA seq even though they could be detected in the controls. Further analysis revealed that those transcripts normally already expressed at high levels were favored for detection in thiophosphate treated samples (see Table 1).

**Table 1.** Results compare the natural abundance of *E. coli* mRNA<sup>9</sup> with their ability to be detected via RNA seq in samples from bacteria grown in thiophosphate.

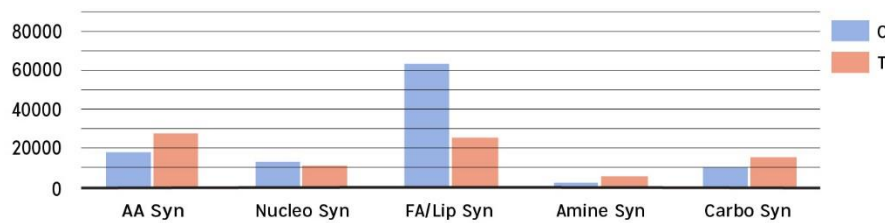
Abundance Class mRNA Control	% Detected in Treated mRNA
>3 QRT	60%
>Median	50.5%
<Median	16%

### BIOSYNTHETIC PATHWAYS

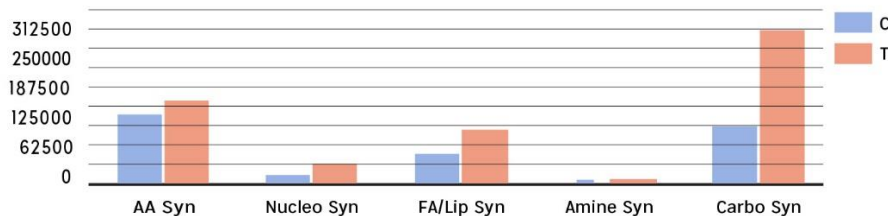
Omics analysis of general biosynthetic pathways revealed a reduction in fatty acid/lipid synthesis and cofactor synthesis in thiophosphate treated cells compared with controls at 1 hr. (Fig 2). In contrast amino acid synthesis and carbohydrate synthesis were elevated (Fig 2). However, looking more specifically at the pathways, mRNA transcripts for saturated and unsaturated fatty acid synthesis were impacted the most. This contrasts with late log where transcripts for all these synthetic pathways are

enhanced as shown in Fig. 2 and previous work<sup>1</sup>. For carbohydrate synthesis, the increases at 1 hr. after treatment were mostly in glycan synthesis (some glycogen and starch) and in the sugar nucleotide synthesis pathways (Fig 3). This contrasts with late log where there is a small increase in transcripts for the gluconeogenesis pathway and a significant increase in transcripts for the trehalose synthesis pathways. Late log also shows an apparent 19X fold increase in transcripts for glucan and glycogen/starch synthesis<sup>1</sup>.

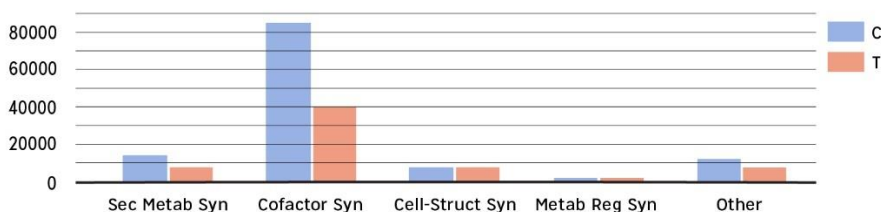
A



B



C



D

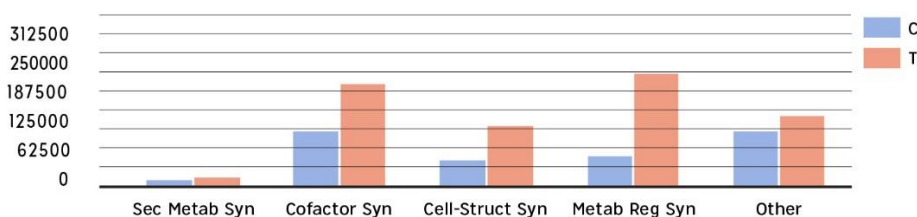


**Figure 2.** RNA seq counts (FPKM) from control samples shown in blue and thiophosphate treated samples in red. Panels A and C are from cells grown for 1 hr., while panels B and D are from cells grown to late log. The values for panels B and D are adjusted 25X fold to account for the presence of rRNA in samples and aide in comparison.

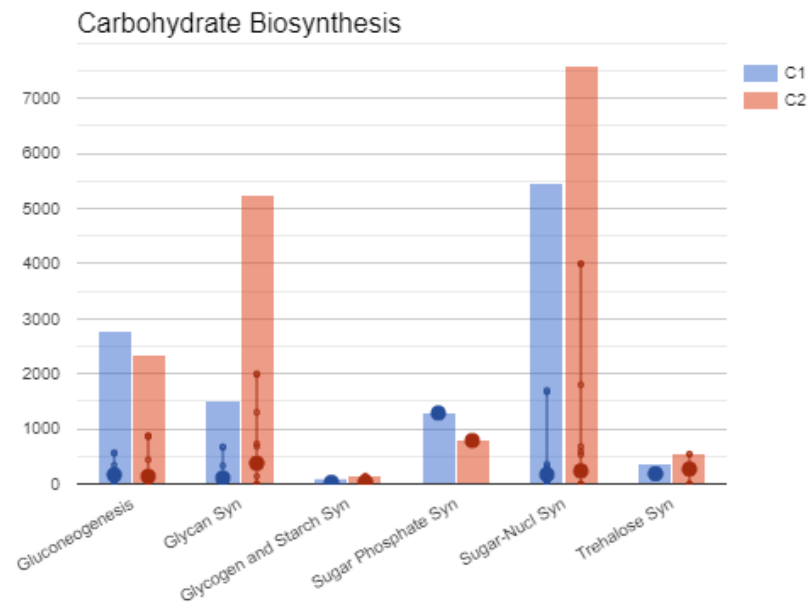


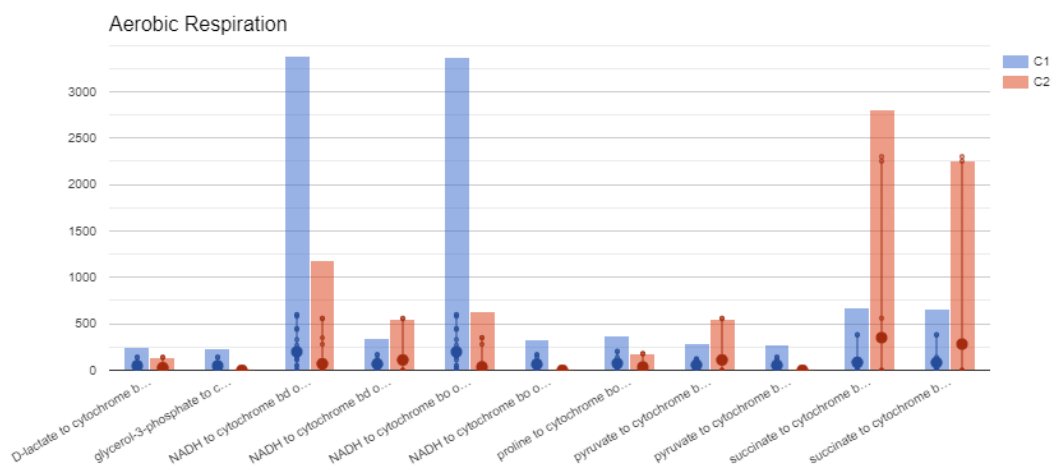
**Figure 3.** 1 hr. RNA seq counts (FPKM) from control samples shown in blue and thiophosphate treated samples in red.

#### ENERGY PATHWAYS

Omics analysis of energy pathways revealed that early on there is a 3X fold increase in transcripts for TCA cycle genes, a slight increase in fermentation gene transcripts, and a decrease in anaerobic gene pathway transcripts. Further analysis showed that the increase is largely in succinate to cytochrome bo

and bd pathways with a decrease in NADH to cytochrome bd and bo pathways (Fig. 4A). This contrasts with late log where things are generally elevated but pyruvate to cytochrome bo and bd pathways dramatically so while, succinate to cytochrome bo and bd are still elevated but less so (Fig. 4B).

A



B

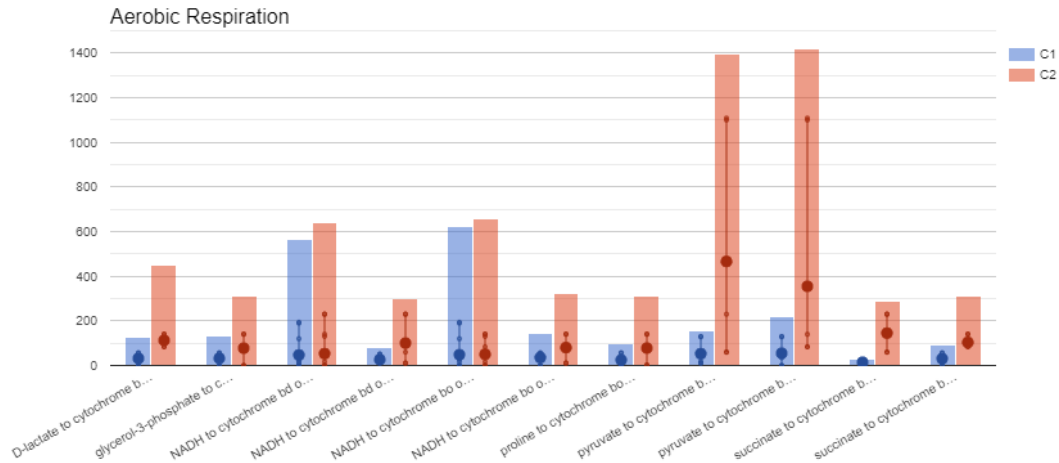


**Figure 4.** RNA seq counts (FPKM) in control samples shown in blue and thiophosphate treated samples in red. 4A shows results from 1 hr. samples and B from late log samples. Note, the late log data was obtained using total RNA without removing ribosomal RNA reads. To make the signal more comparable multiple late values by ~25X.

#### EARLY ACTIVATED GENES

Table 2 shows a list of some genes whose transcripts were enhanced at the 1 hr. time point using thiophosphate relative to control cells. Also shown are late log results for comparison. Interestingly, the most enhanced is a potential epigenetic regulator

corresponding to the *yegI* gene which encodes a ser/thr kinase. Although not as highly upregulated, another epigenetic regulator was detected, *Yafs*, a methyltransferase whose transcripts were enhanced ~14.5X fold in thiophosphate treated cells.

**Table 2.** Changes in transcript levels for genes in thiophosphate treated cells relative to controls. ND not detected. – signal too high to quantitate.

Gene	Fold Increase 1 hr	Fold Increase Late Log	Function
<i>yegI</i>	190	ND	Ser/Thr Kinase
<i>waaU</i>	104	--	ADP heptose transfer
<i>ilvG</i>	87	--	Isoleucine syn with frameshift mutation
<i>arpA</i>	81	--	Reg acetyl CoA syn
<i>argD</i>	75	ND	Arg/Lys syn
<i>ybiA</i>	70	ND	Flavin biosynthesis
<i>rseB</i>	56	--	Sigma E neg regulator
<i>hisI</i>	54	5	His biosynthesis
<i>ygaQ</i>	52	ND	Interrupted gene
<i>cysS</i>	43	1.4	Cys-tRNA ligase
<i>rluc</i>	43	1.2	23S rRNA pseudo uridine synthase
<i>proC</i>	41	0	Proline syn

### GC RICH SEQUENCES IN THIOPHOSPHATE TREATED CELLS

Fasta GC analysis revealed a bimodal distribution in the GC content of thiophosphate treated RNA (Fig. 5). While the bulk sequence was normal at 51% GC, a separate peak was observed with a GC content of 73-74%. While GC islands at that

GC content level are not common, a few were detected >130 bp with 72% or more GC content in gene sequences. Of the genes detected only *phnI*, *phnH*, *phnP*, and *rhsB* had transcripts that were elevated in thiophosphate treated cells. *PhnI* was increased the most at ~48X fold. No comparable GC islands were detected in intergenic regions.

### FastQC: Per Sequence GC Content

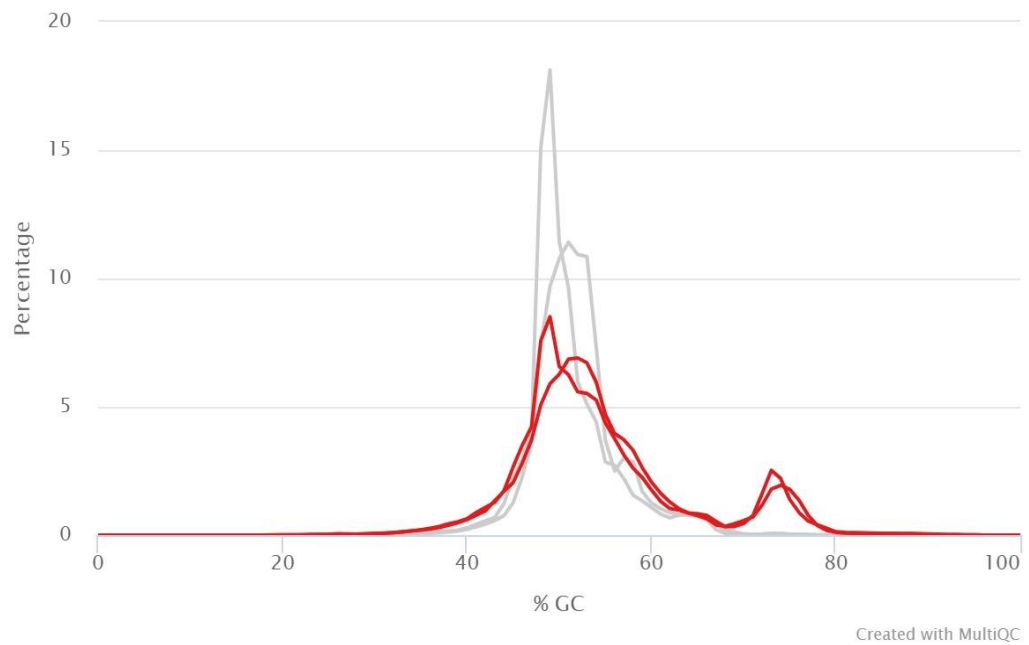


**Figure 5.** The red line shown corresponds to RNA isolated from thiophosphate treated cells while the grey line represents RNA isolated from control cells.

### FastQC: Sequence Duplication Levels

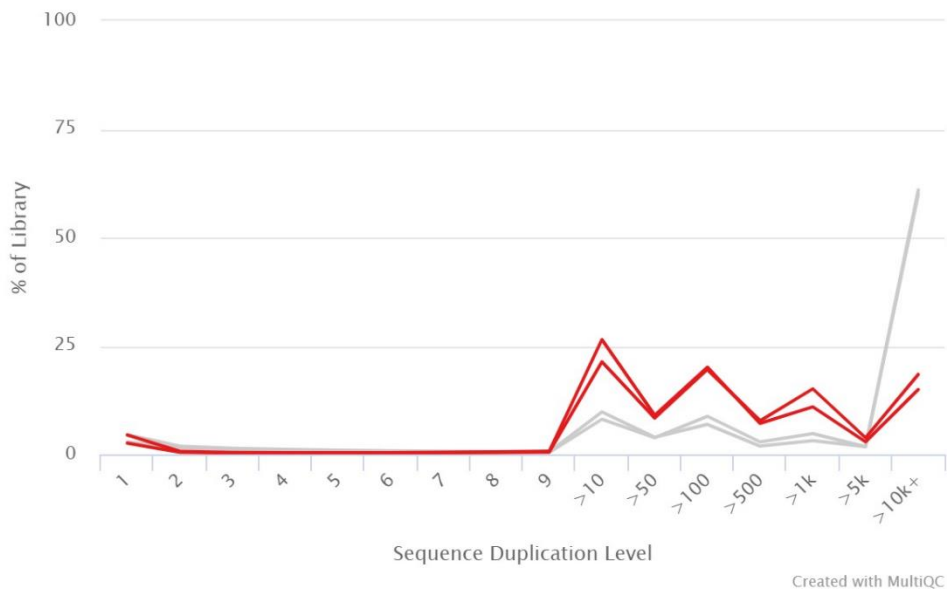


**Figure 6.** RNA sequence FastQC sequence duplication results. Red line corresponds to results using RNA isolated from thiophosphate treated cells and grey to control cells.

### BULK SHIFT IN NON-RIBOSOMAL RNA

Fasta analysis of sequence duplication levels showed a decrease in certain RNAs present at more than 5000 copies in the control library (Fig. 6). As rRNA was depleted prior to RNA seq analysis, this RNA most likely represents tmRNA as it is not removed. tmRNA has structural features like tRNA (and mRNA) and is very stable<sup>10</sup>. Enrichment of bulk mRNA in thiophosphate treated cells was expected as it is much less stable than ribosomal RNA and accumulates due to the incorporation of phosphorothioate linkages. Fig. 6 shows increases in three peaks representing abundant mRNA species that were further increased in thiophosphate treated cells.

### Discussion

The induction of biosynthesis in *E. coli* by thiophosphate serves as a potential model of metabolic induced differentiation<sup>2</sup>. In this case an increase in cellular energy and possibly the cellular energy charge is proposed to serve as the trigger of increased biosynthetic activity. A target of this activity that could serve to mediate in signaling is the *yegI* protein, a known ser/thr kinase that was activated 190X at the mRNA level during the initial phase of the developmental response. The *yegI* protein is a putative transmembrane protein with both N and C termini located intracellularly, consistent with a potential to respond to intracellular events as opposed to extracellular stimuli<sup>11</sup>. This raises the possibility that the enzyme could be activated directly in the cytosol or indirectly via changes in the cell membrane to undergo autophosphorylation in response to changes in the energy state of the cell. Currently, the activation signals for such protein kinases are not understood. *YegI* could presumably participate in initiating the transcription of other gene targets and even itself via the phosphorylation of regulatory molecules. Although his and asp phosphorylation is more common in bacteria, ser/thr phosphorylation is common in eukaryotes and the *yegI* gene based on sequence homology, is a eukaryote-like ser/thr kinase, also called an STPK<sup>12</sup>.

Another potential candidate in mediating thiophosphate induced changes is *Yafs*, a putative S-adenosyl methionine dependent methyltransferase, which is upregulated 14X fold. These enzymes methylate a broader range of entities from metabolites to biomolecules<sup>13</sup>. Methylation is known to play a role in the regulation of gene expression, although it is usually negative. However, this might be helpful in negatively regulating transcription under conditions of unbridled levels of transcripts. Note, the level of SAM can be limiting for methyltransferase activity,

which can be enhanced with increased methionine in bacteria<sup>14</sup>. Interestingly, the *metH* gene involved in methionine biosynthesis was elevated 2.5X fold in thiophosphate treated cells.

The present findings indicate that the bulk of non-ribosomal RNA was stabilized relative ribosomal RNA in thiophosphate treated cells at 1 hr. due to the incorporation of nuclease resistant phosphorothioate linkages in RNA. This was seen directly in total RNA samples run on Agilent gels in Fig 1 showing extra bands as well as from corresponding digital scans of the gels. Also, the Fasta sequence data in Fig 5. showed an increase in presumably mRNA relative to tmRNA. The impact on non-ribosomal RNA accumulation appeared to reach steady state by ~5 hrs. of incubation in the thiophosphate substituted media. The associated changes in transcript levels at one hr. are unlikely due to differences in RNA stability. This is suggested from previous work of late log samples where no correlation between changes in gene expression and RNA stability is observed. Similarly at 1 hr. of incubation, 6 out of the 8 genes in Table 2 for which half-life data are available<sup>15</sup>, did not have short half-lives. *yegI* has a nearly typical half-life of 5.5 minutes in M9 media and *yafs* as long as 4 minutes.

The one hr. early time point is likely to have a much greater fraction of mRNAs increased than seen in Table 2, albeit by lower amounts closer to the average of 8-10X fold. This is because with the massive increase in non-ribosomal RNA brought on by the phosphate analogue, many genes detected in the control were not detected in TP samples (Table 1). Thirty of the 157 gene sequences that were reduced in thiophosphate treated samples were reduced by 5X fold or more. Consistent with a reduction in fatty acid synthesis and cofactor synthesis were decreases in the transcripts for *fabA* and *dxs*, even though they both increase later. Reductions in *rpsA*, *rlmN*, *rsmC* transcripts in thiophosphate treated cells suggest reduced processing of rRNA and possibly translation, which are both also increased at later time points.

The possible reduction in NADH to cytochrome bd and bo oxidases during the first hour of thiophosphate induction is intriguing (Fig. 4A). It may be because there is initially less need for ATP production via the electron transport chain with the energy savings from reduced RNA turnover. As biosynthesis increases at later stages, the levels of transcripts for the NADH bd and bo oxidase genes return to normal (Fig. 4B). Alternatively, the cells may already be preparing to conserve NADH for NADPH production. The increased levels of transcripts in succinate to bd and bo oxidases genes



may be a way to generate energy, and especially in later stages, serve to help preserve carbon sources for biosynthetic activity as well. In this regard, the enhanced pyruvate to bd and bo oxidase pathway seen in late thiophosphate treated cells is not overall energetically favorable as it results in acetate not acetyl CoA. Overall, the results are consistent with the idea that reduced RNA turnover in thiophosphate treated cells increases the cellular energy charge or state leading to the activation of a protein

phosphorylation cascade via yegl to enact the new transcriptional program.

**Conflict of Interest:** The author declares no conflicts of interest.

**Funding:** None.

**Acknowledgements:** I wish to thank Wenzhi Li, M.D. of Omega Bioservices for helping with the RNA Seq study.

## References

1. Frayne EG. Global profile changes in transcripts induced with a phosphate analogue: implications for gene regulation. *Molecular and Cellular Biochemistry*. 2020;468(1-2):111. doi:10.1007/s11010-020-03715-9
2. Frayne E. Metabolic Regulation of Cell Differentiation. *Advanced Chemobiology Research*. Published online November 4, 2020:1-4. doi:https://doi.org/10.37256/acbr.112022543
3. Nowak-Stepniowska A, Osuchowska PN, Fiedorowicz H, Trafny EA. Insight in Hypoxia-Mimetic Agents as Potential Tools for Mesenchymal Stem Cell Priming in Regenerative Medicine. *Stem Cells International*. March 2022:1-24. doi:10.1155/2022/8775591
4. Yu J-Z, Wang J, Sheridan SD, Perlis RH, Rasenick MM. N-3 polyunsaturated fatty acids promote astrocyte differentiation and neurotrophin production independent of cAMP in patient-derived neural stem cells. *Molecular Psychiatry*. 2021;26(9):4605. doi:10.1038/s41380-020-0786-5
5. Persad KL, Lopaschuk GD. Energy Metabolism on Mitochondrial Maturation and Its Effects on Cardiomyocyte Cell Fate. *Front Cell Dev Biol*. 2022;10:886393. Published 2022 Jul 5. doi:10.3389/fcell.2022.886393
6. Agilent Technologies Agilent High Sensitivity RNA ScreenTape System Quick Guide. Accessed January 5, 2024. [https://www.agilent.com/cs/library/usermanuals/public/ScreenTape\\_HSRNA\\_QG.pdf](https://www.agilent.com/cs/library/usermanuals/public/ScreenTape_HSRNA_QG.pdf)
7. Keseler IM, Mackie A, Santos-Zavaleta A, et al. The EcoCyc database: reflecting new knowledge about Escherichia coli K-12. *Nucleic acids research*. 2017;45(D1):D543-D550. doi:10.1093/nar/gkw1003
8. Kuznetsov A, Bollin CJ. NCBI Genome Workbench: Desktop Software for Comparative Genomics, Visualization, and GenBank Data Submission. *Methods in Molecular Biology*. Published online December 9, 2020:261-295. doi:https://doi.org/10.1007/978-1-0716-1036-7\_16
9. Taniguchi Y, Choi PJ, Li GW, et al. Quantifying E. coli proteome and transcriptome with single-molecule sensitivity in single cells [published correction appears in Science. 2011 Oct 28;334(6055):453]. *Science*. 2010;329(5991):533-538. doi:10.1126/science.1188308
10. Hudson CM, Williams KP. The tmRNA website. *Nucleic Acids Research*. 2014;43(D1):D138-D140. doi:https://doi.org/10.1093/nar/gku1109
11. Rajagopalan K, Dworkin J. Escherichia coli Yegl is a novel Ser/Thr kinase lacking conserved motifs that localizes to the inner membrane. *FEBS Letters*. 2020;594(21):3530-3541. doi:https://doi.org/10.1002/1873-3468.13920
12. Nagarajan SN, Lenoir C, Grangeasse C. Recent advances in bacterial signaling by serine/threonine protein kinases. *Trends in Microbiology*. 2022;30(6):553-566. doi:10.1016/j.tim.2021.11.005
13. Sánchez-Romero MA, Casadesús J. The bacterial epigenome. *Nature Reviews Microbiology*. 2019;18(1):7-20. doi:https://doi.org/10.1038/s41579-019-0286-2
14. Liu Q, Lin B, Tao Y. Improved methylation in E. coli via an efficient methyl supply system driven by betaine. *Metabolic Engineering*. 2022;72:46-55. doi:https://doi.org/10.1016/j.ymben.2022.02.004
15. Bernstein JA, Khodursky AB, Lin PH., Lin-Chao S, Cohen SN. Global analysis of mRNA decay and abundance in Escherichia coli at single-gene resolution using two-color fluorescent DNA microarrays. *Proceedings of the National Academy of Sciences*. 2002;99(15):9697-9702. doi:https://doi.org/10.1073/pnas.112318199